ELSEVIER

Engineering Analysis with Boundary Elements 27 (2003) 789–802

ENGINEERING ANALYSIS *with* BOUNDARY ELEMENTS

www.elsevier.com/locate/enganabound

A complex boundary integral method for multiple circular holes in an infinite plane

Jianlin Wang, Steven L. Crouch, Sofia G. Mogilevskaya*

Department of Civil Engineering, University of Minnesota, 500 Pillsbury Drive SE, Minneapolis, MN 55455, USA

Received 21 August 2002; revised 15 January 2003; accepted 28 January 2003

Abstract

A complex boundary integral equation method, combined with series expansion technique, is presented for the problem of an infinite, isotropic elastic plane containing multiple circular holes. Loading is applied at infinity or on the boundaries of the holes. The sizes and locations of the holes are arbitrary provided they do not overlap. The analysis procedure is based on the use of a complex hypersingular integral equation that expresses a direct relationship between all the boundary tractions and displacements. The unknown displacements on each circular boundary are represented by truncated complex Fourier series, and all of the integrals involved in the complex integral equation are evaluated analytically. A system of linear algebraic equations is obtained by using a Taylor series expansion, and the block Gauss–Seidel algorithm is used to solve the system. Several numerical examples are considered to demonstrate the accuracy, versatility, and efficiency of the approach.

Keywords: Complex boundary integral equation method; Multiple circular holes; Complex hypersingular integral equation; Complex Fourier series; Taylor series expansion; Galerkin method

1. Introduction

The problem of calculating the displacement and stress fields in an elastic body containing an assortment of holes is of considerable interest in engineering. Among other applications, this problem is important in understanding the mechanical behavior of perforated solids and determining their effective elastic properties. Particular situations may involve large numbers of regularly or randomly distributed holes, some of which might be closely spaced. A general method to tackle the problem should therefore allow one to effectively and accurately calculate the interactions among multiple holes with arbitrary sizes and locations.

A number of numerical methods have been developed for solving problems involving multiple holes (and also elastic inclusions) in an infinite elastic solid. Excluding differential methods (e.g. finite elements), these can be classified as series expansion methods, boundary integral equation methods, or a combination of the two. Special variants of these approaches have been devised for periodic arrays of holes [1,2], but we are concerned here only with randomly distributed holes of different sizes. We are also concerned with the special (but practically very important) case in which all of the holes are circular.

Early attempts to solve problems involving multiple, randomly distributed circular holes using series expansions are reported by Green [3], Yu [4], and Yu and Sendeckyj [5]. Green solved the problem by expanding Airy's stress function into a Fourier series whose unknown coefficients were themselves represented by infinite series. For the case of three holes in a row, Green proved that his method converged provided the holes were well separated. He was, however, unable to obtain any general conditions of convergence for arbitrary hole sizes and locations. To our knowledge, no attempts have been made to implement Green's method on a modern-day digital computer.

Yu [4] and Yu and Sendeckyj [5] considered the more general problem of multiple randomly distributed circular inclusions and treated a hole as the limiting case of an inclusion with zero shear modulus. Their numerical technique was based on the singular solution (in the form of series expansions of the Kolosov–Muskhelishvili

* Corresponding author. Tel.: +1-612-625-4810; fax: +1-612-626-7750.
E-mail address: mogil003@tc.umn.edu (S.G. Mogilevskaya).

0955-7997/03/$ - see front matter © 2003 Elsevier Ltd. All rights reserved.
doi:10.1016/S0955-7997(03)00043-2

potentials) for an infinite plane containing a circular inclusion, together with an implementation of Schwarz's alternating method [6]. The authors claimed that the number of inclusions and their locations and elastic properties were arbitrary, but the convergence of their algorithm was found to be poor if the inclusions were close together or if more than a few inclusions were present. It appears that Yu and Sendeckyj did not pursue this work beyond their initial investigations.

More recently, Ting et al. [7] described an alternating method for analyzing the interactions among multiple circular holes. Their method is based on the analytical solution to the problem of an infinite plane containing a single circular hole subjected to arbitrary boundary tractions represented as truncated Fourier series. A problem involving multiple holes is solved by an iterative superposition process in which each hole is treated as an isolated entity whose boundary conditions are specified in terms of the effects of all of the other holes. The authors do not explicitly state whether they used numerical or analytical integration to obtain the Fourier coefficients that account for the hole to hole interactions.

Meguid and Shen [8] and Gong and Meguid [9] used a series expansion approach to treat the problem of multiple randomly distributed circular holes and inclusions in an infinite plane. In their approach, the Kolosov–Muskhelishvili potentials are represented as Laurent series. The boundary conditions for the problem are used to obtain an infinite system of linear algebraic equations whose unknown coefficients are further expanded into infinite series with respect to a characteristic parameter that depends on the relative distances between the circular holes or inclusions. Similar to Green's [3] approach, the use of double series introduces an additional computational cost and makes convergence difficult to achieve for closely spaced inclusions and holes. In addition, the algorithm is dependent on the choice of the characteristic parameter.

The second general approach for solving problems involving multiple, randomly distributed circular holes is to use a boundary integral equation method. Most investigators use Fourier series approximations for the unknowns in the boundary integral equation [10,11], but it is also possible to use a conventional boundary element method in which the boundary is subdivided into elements and the unknowns are approximated in piecewise fashion by polynomials, i.e. by collocation [12,13]. The latter approach, of course, is applicable to boundaries of arbitrary shape. Interestingly, apart from our own work [14,15], all of the papers that we have been able to find on boundary element solutions of the multiple hole problem employ indirect boundary element formulations in which the unknowns in the governing integral equations (typically a density function of some kind) do not have a clear physical meaning.

For example, Horii and Nemat-Nasser [10] presented a general technique for circular holes called the 'method of pseudotractions.' This method is based on the solution of a system of boundary integral equations with the unknown pseudotractions expressed as complex Fourier series. A system of algebraic equations for the Fourier coefficients is obtained analytically, ensuring that the surfaces of the holes are traction free. Horii and Nemat-Nasser's examples are restricted to two or three randomly spaced holes or a row of periodically spaced holes, and they do not address the issue of how to choose the number of terms in the Fourier series.

Duan et al. [11] developed an approach that combines the boundary integral method with series expansions to treat problems involving circular holes. They obtained a system of complex boundary integral equations for holes using a complex analog of the body force method [16]. A comparison was made for a simple case of two symmetrically located holes using a conventional boundary element method with collocation and a method using Fourier series expansions for the unknown body force densities. Duan et al. found that the asymptotic behavior for the hole-to-hole interactions is similar to that of stress behavior near a crack tip, and that the conventional boundary element method is not effective in capturing this behavior, even for the case of two closely spaced holes. They concluded that the series expansion technique is superior to the conventional boundary element method when the holes are very close together. Duan et al. [11] did not notice that all integrations in their series expansion approach could be done analytically; instead, they calculated regular integrals numerically using Simpson's rule.

Helsing and Jonsson [13] combined an indirect boundary element technique with a fast multipole method [17–19] to treat large-scale problems with holes of arbitrary shapes. They considered the special case of circular holes in their work, but the circular boundaries were treated as ordinary boundary elements, divided into a large number of discretization points, and no special representation was used for the density function in their boundary integral equation. Greengard and Helsing [12] used a similar approach to solve problems with inclusions of various shapes, including circular inclusions. The integral equation used for their work is applicable to two-component materials only, and is not valid for the case in which the shear modulus of the inclusion phase is zero, i.e. for holes. For circular inclusions, the authors mention that the density function in their integral equation can be represented as a Fourier series and that all integrations can be done analytically, but they do not give any details.

In the present paper we combine a series expansion approach with a direct boundary element formulation to solve the problem of multiple circular holes in an infinite elastic plane. A similar approach was presented by Mogilevskaya and Crouch [14] for an infinite plane with an arbitrary number of randomly distributed, perfectly bonded circular elastic inclusions with arbitrary elastic properties; subsequently, this approach was extended to include inclusions with homogeneously imperfect interfaces

[15]. Both types of problems—holes and inclusions—are governed by a complex hypersingular boundary integral equation [20] that expresses a direct relationship between boundary displacements (or displacement discontinuities) and tractions. For problems involving perfectly bonded inclusions, the displacement discontinuities are equal to zero and the tractions on the boundaries of the inclusions are unknown; for holes, the tractions are known and the displacement discontinuities (which are equal to the displacements on the boundaries of the holes) are unknown. In applying Linkov and Mogilevskaya's complex hypersingular boundary integral equation, therefore, separate analyses are required for inclusions and holes. In particular, a hole cannot simply be viewed as a limiting case of an inclusion with zero shear modulus but must be treated separately.

In the work described here, the boundary displacements are approximated by truncated complex Fourier series, which are uniformly convergent provided the holes do not overlap. We take advantage of the circular geometry and perform all of the integrations in the complex hypersingular boundary integral equation analytically. Using Taylor series expansions, a system of linear algebraic equations is set up to obtain the unknown Fourier coefficients. No double series are involved in our method, and the matrix of the linear algebraic system has diagonal submatrices on its diagonal, which allows the system to be effectively solved using a block Gauss–Seidel iterative method. The iterative procedure also allows one to determine the number of terms of the Fourier series needed to reach a specified accuracy level. Several numerical examples are given to demonstrate the accuracy and effectiveness of this approach.

2. Problem description

We consider an infinite elastic body containing an arbitrary assortment of N nonoverlapping circular holes (Fig. 1). The holes are assumed to be either traction-free or subjected to constant normal traction. The entire region is subjected to an arbitrarily oriented uniform stress field at infinity. The shear modulus and Poisson's ratio for the material are μ and υ, respectively. Let R_j, z_j, and L_j denote the radius, center, and boundary of the jth hole, and let p_j denote the constant normal traction acting on L_j ($p_j < 0$ for compression). Any point of the plane is identified by the complex coordinate $z = x + iy$. The global and local Cartesian coordinate systems are shown in Fig. 1. The direction of travel is clockwise for all the boundaries L_j. The unit tangent s points in the direction of travel and the unit outward normal n points to the right of this direction, away from the solid. The distribution of displacements and stresses in the perforated solid are to be determined.

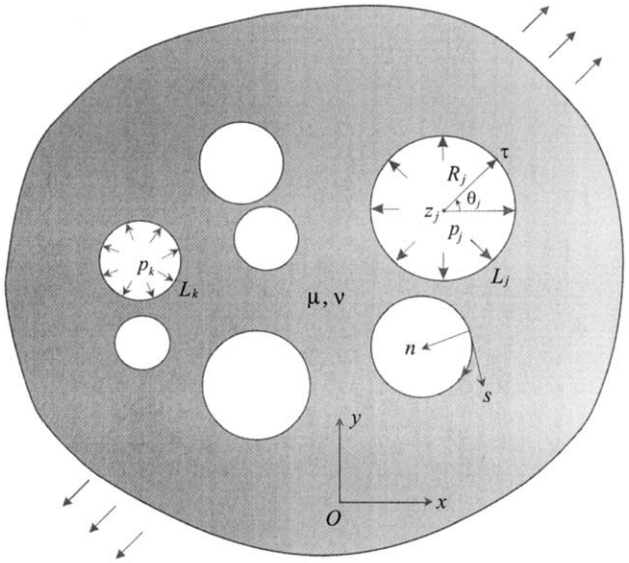

Fig. 1. Problem formulation.

3. Boundary integral equation

We start with a complex hypersingular integral equation that was originally developed by Linkov and Mogilevskaya [20]. We showed in detail in Ref. [14] that this equation has advantages over the singular and regular integral equations available in the literature for similar kinds of problems. The use of complex integral equations has proven its superiority in solving two-dimensional potential and elasticity problems (see, for example, Hromadka [21] and Chen and Chen [22]). After reformulation, the complex hypersingular integral equation for the present problem can be written as follows:

$$\frac{1}{2\pi i}\sum_{j=1}^{N}\left\{2\int_{L_j}\frac{u_j(\tau)}{(\tau-t)^2}d\tau-\int_{L_j}u_j(\tau)\frac{\partial^2}{\partial\tau\partial t}K_1(\tau,t)d\tau\right.$$
$$-\int_{L_j}\overline{u_j(\tau)}\frac{\partial^2}{\partial\bar{\tau}\partial t}K_2(\tau,t)d\bar{\tau}+\frac{p_j}{2\mu}\left[(1-\kappa)\int_{L_j}\frac{d\tau}{\tau-t}\right.$$
$$\left.\left.-\kappa\int_{L_j}\frac{\partial}{\partial t}K_1(\tau,t)d\tau+\int_{L_j}\frac{\partial}{\partial t}K_2(\tau,t)d\bar{\tau}\right]\right\}$$
$$=\frac{\kappa+1}{4\mu}\left[p_k-(\sigma^{\infty}_{xx}+\sigma^{\infty}_{yy})-\frac{d\bar{t}}{dt}(\sigma^{\infty}_{yy}-\sigma^{\infty}_{xx}-2i\sigma^{\infty}_{xy})\right],$$
$$t\in L_k\,(k=1,2,\ldots,N) \qquad (1)$$

where $u_j=(u_x)_j+i(u_y)_j$ are the complex-valued displacements in the global coordinate system on the boundary of the jth hole; σ^{∞}_{xx}, σ^{∞}_{yy}, and σ^{∞}_{xy} are the stresses at infinity; $\kappa=3-4\upsilon$ for plane strain or $\kappa=(3-\upsilon)/(1+\upsilon)$ for plane stress; $d\bar{t}/dt=\exp(-2i\beta)$ and β is the angle between the axis Ox and the tangent at the point t; and the kernels K_1 and K_2 are

$$K_1(\tau,t)=\ln\frac{\tau-t}{\bar{\tau}-\bar{t}};\ K_2(\tau,t)=\frac{\tau-t}{\bar{\tau}-\bar{t}}$$

Eq. (1) is written directly in terms of the displacements and tractions on the boundaries. In our case, the tractions are known and the unknown displacements are to be determined. The stresses and displacements at any point z inside the solid can be calculated from the boundary values of displacements and tractions by using the Kolosov–Muskhelishvili formulae [23]

$$u_x(z)+\mathrm{i}u_y(z)=\frac{1}{2\mu}\left[\kappa\varphi(z)-z\overline{\varphi'(z)}-\overline{\psi(z)}\right]$$
$$\sigma_{xx}+\sigma_{yy}=4\,\mathrm{Re}\,\varphi'(z)$$
$$\sigma_{yy}-\sigma_{xx}+2\mathrm{i}\sigma_{xy}=2[\bar{z}\varphi''(z)+\psi'(z)] \tag{2}$$

where the two potentials $\varphi(z)$ and $\psi(z)$ can be can be written in the form of integral equations as [24]

$$\varphi(z)=\frac{\mu}{\pi\mathrm{i}(\kappa+1)}\sum_{j=1}^{N}\int_{L_j}\frac{u_j(\tau)}{\tau-z}\mathrm{d}\tau+\varphi^{\infty}(z)$$

$$\psi(z)=-\frac{\mu}{\pi\mathrm{i}(\kappa+1)}\sum_{j=1}^{N}\left\{\frac{p_j}{2\mu}\left[\int_{L_j}\frac{\bar{\tau}\mathrm{d}\tau}{\tau-z}+\kappa\int_{L_j}\ln(\tau-z)\mathrm{d}\bar{\tau}\right]+\int_{L_j}\frac{\overline{u_j(\tau)}}{\tau-z}\mathrm{d}\tau-\int_{L_j}\frac{u_j(\tau)}{\tau-z}\mathrm{d}\bar{\tau}+\int_{L_j}\frac{u_j(\tau)\bar{\tau}}{(\tau-z)^2}\mathrm{d}\tau\right\}+\psi^{\infty}(z) \tag{3}$$

where

$$\varphi^{\infty}(z)=\frac{\sigma_{xx}^{\infty}+\sigma_{yy}^{\infty}}{4}z$$

$$\psi^{\infty}(z)=\frac{\sigma_{yy}^{\infty}-\sigma_{xx}^{\infty}+2\mathrm{i}\sigma_{xy}^{\infty}}{2}z$$

4. Numerical solution

4.1. Complex Fourier series representation

In order to solve the hypersingular integral Eq. (1), we expand the unknown displacement $u_j(\tau)$ on the circular boundary L_j by truncated complex Fourier series as

$$u_j(\tau)=D_{0j}+\sum_{m=1}^{M_j}[D_{-mj}\exp(-\mathrm{i}m\theta_j)+D_{mj}\exp(\mathrm{i}m\theta_j)],\ \tau\in L_j \tag{4}$$

where θ_j is the angle between the axis Ox and the vector $\tau-z_j$, and thus we have $\tau-z_j=R_j\exp(\mathrm{i}\theta_j)$. For notational convenience, we define a function $g_j(\tau)$ as follows,

$$g_j(\tau)=\frac{R_j}{\tau-z_j} \tag{5}$$

Representation (4) can then be rewritten as

$$u_j(\tau)=D_{0j}+\sum_{m=1}^{M_j}[D_{-mj}g_j^{m}(\tau)+D_{mj}g_j^{-m}(\tau)],\ \tau\in L_j \tag{6}$$

The complex coefficients $D_{\pm mj}$ $(m=1,\ldots,M_j)$ and D_{0j} involved in the above series expansions need to be determined. This can be done by setting up and solving a simultaneous, linear algebraic equations, as described below. We note that the number of terms needed in the series expansion for each hole is also unknown and is not necessarily the same for all the individual holes.

4.2. Evaluation of the integrals and resulting equations

Based on the above representations of the unknown displacements on the boundaries, all the integrals in Eq. (1) can be evaluated analytically by using the Cauchy integral theorem and the residue theorem. The procedure for calculating these integrals is similar to that in Mogilevskaya and Crouch [14], and thus only the results are given here. If the evaluation point t is on boundary L_k, then substitution of approximation (6) into Eq. (1) yields the following results for the first three integrals involving the unknown displacements:

$$\mathscr{I}_1=\int_{L_j}\frac{u_j(\tau)}{(\tau-t)^2}\mathrm{d}\tau=\begin{cases}-\dfrac{\pi\mathrm{i}}{R_k}\displaystyle\sum_{m=1}^{M_k}m[D_{-mk}g_k^{m+1}(t)+D_{mk}g_k^{1-m}(t)], & j=k\\ -\dfrac{2\pi\mathrm{i}}{R_j}\displaystyle\sum_{m=1}^{M_j}mD_{-mj}g_j^{m+1}(t), & j\neq k\end{cases} \tag{7}$$

$$\mathscr{I}_2=\int_{L_j}u_j(\tau)\frac{\partial^2}{\partial\tau\partial t}K_1(\tau,t)\mathrm{d}\tau=\begin{cases}0, & j=k\\ -\dfrac{2\pi\mathrm{i}}{R_j}\displaystyle\sum_{m=1}^{M_j}m[D_{-mj}g_j^{m+1}(t)-D_{mj}g_k^{2}(t)\overline{g_j^{m+1}(t)}], & j\neq k\end{cases} \tag{8}$$

$$\mathscr{I}_3=\int_{L_j}\overline{u_j(\tau)}\frac{\partial^2}{\partial\bar{\tau}\partial t}K_2(\tau,t)\mathrm{d}\bar{\tau}=\begin{cases}2\pi\mathrm{i}\dfrac{\bar{D}_{1k}}{R_k}, & j=k\\ \dfrac{2\pi\mathrm{i}}{R_j}\left\{\displaystyle\sum_{m=1}^{M_j}m\bar{D}_{-mj}\left[\overline{g_j^{m+1}(t)}-(m+2)g_k^{2}(t)\overline{g_j^{m+3}(t)}+(m+1)\overline{g_j^{m+2}(t)}\frac{g_k^{2}(t)}{g_j(t)}\right]+\bar{D}_{1j}g_k^{2}(t)\overline{g_j^{2}(t)}\right\}, & j\neq k\end{cases} \tag{9}$$

Similarly, another three integrals involving the known tractions on boundaries L_j can easily be calculated,

$$\mathscr{I}_4=\int_{L_j}\frac{\mathrm{d}\tau}{\tau-t}=\begin{cases}-\pi\mathrm{i}, & j=k\\ 0, & j\neq k\end{cases} \tag{10}$$

$$\mathscr{I}_5=\int_{L_j}\frac{\partial}{\partial t}K_1(\tau,t)\mathrm{d}\tau=\begin{cases}0, & j=k\\ 2\pi\mathrm{i}g_k^2(t)\overline{g_j^2(t)}, & j\neq k\end{cases} \tag{11}$$

$$\mathscr{I}_6=\int_{L_j}\frac{\partial}{\partial t}K_2(\tau,t)\mathrm{d}\bar{\tau}=\begin{cases}-2\pi\mathrm{i}, & j=k\\ -2\pi\mathrm{i}g_k^2(t)\overline{g_j^2(t)}, & j\neq k\end{cases} \tag{12}$$

Upon substitution integrals $\mathscr{I}_1$ through $\mathscr{I}_6$ into Eq. (1), we obtain a system of N complex algebraic equations (one equation for each hole), which are given as follows for the case where evaluation point t is on the boundary $L_k\,(k=1,2,\ldots,N)$,

$$\begin{aligned}&\sum_{m=1}^{M_k}mD_{-mk}g_k^{m+1}(t)+(D_{1k}+\bar{D}_{1k})+\sum_{m=2}^{M_k}mD_{mk}g_k^{1-m}(t)\\&+\sum_{j=1,j\neq k}^{N}\frac{R_k}{R_j}\left\{\sum_{m=1}^{M_j}mD_{-mj}g_j^{m+1}(t)+(D_{1j}+\bar{D}_{1j})g_k^2(t)\overline{g_j^2(t)}\right.\\&+\sum_{m=2}^{M_j}mD_{mj}g_k^2(t)\overline{g_j^{m+1}(t)}\\&+\sum_{m=1}^{M_j}m\bar{D}_{-mj}\left[\overline{g_j^{m+1}(t)}-(m+2)g_k^2(t)\overline{g_j^{m+3}(t)}+(m+1)\right.\\&\left.\left.\times\left(\frac{R_k}{R_j}g_k(t)+\frac{g_k^2(t)}{g_j(z_k)}\right)\overline{g_j^{m+2}(t)}\right]\right\}\\&=\frac{\kappa+1}{4\mu}R_k[\sigma_{xx}^{\infty}+\sigma_{yy}^{\infty}-g_k^2(t)(\sigma_{yy}^{\infty}-\sigma_{xx}^{\infty}-2\mathrm{i}\sigma_{xy}^{\infty})]\\&-\frac{p_k}{\mu}R_k-\frac{1-\kappa}{2\mu}R_kg_k^2(t)\sum_{j=1,j\neq k}^{N}p_j\overline{g_j^2(t)}\end{aligned} \tag{13}$$

Eq. (13) involve $2\sum_{k=1}^{N}M_k$ complex coefficients $D_{\pm mk}\,(m=1,2,\ldots,M_k)$. However, the imaginary parts of D_{1k} are not involved because D_{1k} and $\bar{D}_{1k}$ always come as pairs. Also, it can be seen that the coefficients $D_{0k}\,(k=1,2,\ldots,N)$ do not appear in the system of equations. Although D_{0k} and the imaginary parts of D_{1k} cannot be found from Eq. (13), we will see from Section 4.3 that they can be obtained from the boundary displacements.

4.3. Approximation of the potentials

The Kolosov–Muskhelishvili potentials $\varphi(z)$ and $\psi(z)$ can be obtained by substituting representation (6) into expressions (3). Again, all of the integrals involved in Eq. (3) can be calculated analytically; the results are

$$\begin{aligned}\mathscr{J}_1&=\int_{L_j}\frac{u_j(\tau)}{\tau-z}\mathrm{d}\tau=2\pi\,i\sum_{m=1}^{M_j}D_{-mj}g_j^m(z)\\\mathscr{J}_2&=\int_{L_j}\frac{\bar{\tau}\,\mathrm{d}\tau}{\tau-z}=2\pi\mathrm{i}R_jg_j(z)\\\mathscr{J}_3&=\int_{L_j}\ln(\tau-z)\mathrm{d}\bar{\tau}=-2\pi\mathrm{i}R_jg_j(z)\\\mathscr{J}_4&=\int_{L_j}\frac{\overline{u_j(\tau)}}{\tau-z}\mathrm{d}\tau=2\pi\mathrm{i}\sum_{m=1}^{M_j}\bar{D}_{mj}g_j^m(z)\\\mathscr{J}_5&=\int_{L_j}\frac{u_j(\tau)}{\tau-z}\mathrm{d}\bar{\tau}\\&=-2\pi\mathrm{i}\left[\sum_{m=1}^{M_j}D_{-mj}g_j^{m+2}(z)+D_{1j}g_j(z)\right]\\\mathscr{J}_6&=\int_{L_j}\frac{u_j(\tau)\bar{\tau}}{(\tau-z)^2}\mathrm{d}\tau\\&=-2\pi\mathrm{i}\sum_{m=1}^{M_j}D_{-mj}g_j^m(z)\left[(m+1)g_j^2(z)+m\frac{\bar{z}_j}{z-z_j}\right]\end{aligned} \tag{14}$$

Upon substitution of $\mathscr{J}_1$ through $\mathscr{J}_6$ into Eq. (3), the potentials can therefore be expressed in terms of the values of the complex Fourier coefficients for the displacements at the boundaries of the holes, as follows:

$$\varphi(z)=\frac{2\mu}{\kappa+1}\sum_{j=1}^{N}\sum_{m=1}^{M_j}D_{-mj}g_j^m(z)+\frac{\sigma_{xx}^{\infty}+\sigma_{yy}^{\infty}}{4}z$$

$$\begin{aligned}\psi(z)=&\frac{2\mu}{\kappa+1}\sum_{j=1}^{N}\left[\left(g_j^2(z)+\frac{\bar{z}_j}{z-z_j}\right)\sum_{m=1}^{M_j}mD_{-mj}g_j^m(z)\right.\\&\left.-(D_{1j}+\bar{D}_{1j})g_j(z)-\sum_{m=2}^{M_j}\bar{D}_{mj}g_j^m(z)\right]\\&-\frac{1-\kappa}{1+\kappa}\sum_{j=1}^{N_2}p_jR_jg_j(z)+\frac{\sigma_{yy}^{\infty}-\sigma_{xx}^{\infty}+2\mathrm{i}\sigma_{xy}^{\infty}}{2}z\end{aligned} \tag{15}$$

As can be seen from Eq. (15), the potentials are actually a superposition of the potentials for the individual holes and the potentials arising from tractions on the boundaries of the holes and from the conditions at infinity.

The displacements and stresses at any point inside the material are obtained by substituting the expressions (15) into the Kolosov–Muskhelishvili formulae (2). For the limiting case that the point is on the boundary of hole L_j, the first equation regarding displacements in Eq. (2) is equivalent to representation (6), from which the coefficients D_{0j} and the imaginary parts of D_{1j} can be obtained. It is also observed that D_{0j} and the imaginary parts of D_{1j} are not involved in the potentials and have therefore no

contribution to the stresses and displacements in the matrix.

4.4. Special case of one hole

For the particular case of a single hole L_k, Eq. (13) reduces to the following simple form

$$\sum_{m=1}^{M_k} mD_{-mk}g_k^{m+1}(t) + 2D_{1k} + \sum_{m=2}^{M_k} mD_{mk}g_k^{1-m}(t) = -\frac{p_k}{\mu}R_k + \frac{\kappa+1}{4\mu}R_k[\sigma_{xx}^{\infty} + \sigma_{yy}^{\infty} - g_k^2(t) \times (\sigma_{yy}^{\infty} - \sigma_{xx}^{\infty} + 2\mathrm{i}\sigma_{xy}^{\infty})], \qquad t \in L_k \tag{16}$$

Both sides of this equation represent a truncated complex Fourier series. By comparing the corresponding coefficients of the same power of $g_k(t)$, we obtain the results of the Fourier coefficients for one hole,

$$D_{-1k} = -\frac{\kappa+1}{4\mu}R_k(\sigma_{yy}^{\infty} - \sigma_{xx}^{\infty} + 2\mathrm{i}\sigma_{xy}^{\infty})$$

$$D_{1k} = \frac{\kappa+1}{8\mu}R_k(\sigma_{xx}^{\infty} + \sigma_{yy}^{\infty}) - \frac{p_k}{\mu}R_k$$

$$D_{\pm mk} = 0, \qquad m \geq 2 \tag{17}$$

In this case, the displacements on L_k are exactly represented by a two-term complex Fourier series. Substituting Eq. (17) into Eq. (15) and then using Eq. (2), we get the analytic solution for a circular hole with uniform pressure in an infinite plane subjected to uniform far-field stresses.

4.5. Reduction to a linear algebraic system

In the general case of multiple holes, the solution for the Fourier coefficients in Eq. (13) cannot be obtained as in case of one hole, because the left-hand sides of these equations are no longer represented by a truncated complex Fourier series. A system of linear algebraic equations needs to be formulated to solve for the unknown coefficients. Excluding collocation, there are two ways to reduce Eq. (13) to a linear algebraic system. One way, used in this paper, is to expand all the influence functions $g_j^m(t)$ in Eq. (13) in Taylor series with respect to the evaluation point $t \in L_k$ around the center z_k of a representative hole L_k, such that the left-hand sides of these equations become truncated complex Fourier series. We can accordingly use a similar process to that used in case of one hole to obtain a linear system for the complex Fourier coefficients. Another way to obtain the same system is to use a Galerkin method as described by Mogilevskaya and Crouch [14].

4.5.1. Taylor series expansion

As mentioned above, we decompose all the terms involving the powers of $(t - z_j)$ in a series with respect to $(t - z_k)$ so that Eq. (13) becomes an identity regardless of the location of the evaluation point t. Taking into account that

$$t - z_j = (t - z_k) + (z_k - z_j) = (z_k - z_j)\left(1 + \frac{t - z_k}{z_k - z_j}\right), \qquad t \in L_k \tag{18}$$

we can express functions $g_j^m(t)$ as

$$g_j^m(t) = \frac{R_j^m}{(z_k - z_j)^m\left(1 + \frac{t - z_k}{z_k - z_j}\right)^m} = g_j^m(z_k)\left(1 + \frac{t - z_k}{z_k - z_j}\right)^{-m}, \qquad \left|\frac{t - z_k}{z_k - z_j}\right| < 1 \tag{19}$$

Using the Taylor series expansion

$$(1+x)^{-m} = 1 - mx + \frac{m(m+1)}{2}x^2 + \cdots + (-1)^k\frac{(m+k-1)!}{k!(m-1)!}x^k + \cdots = \sum_{n=0}^{\infty}(-1)^n\binom{m+n-1}{n}x^n, \qquad |x| < 1 \tag{20}$$

where $\binom{m}{n} = m!/[n!(m-n)!]$ are the binomial coefficients, we can write $g_j^m(t)$ and $\overline{g_j^m(t)}$ in series form as

$$g_j^m(t) = g_j^m(z_k)\sum_{n=0}^{\infty}(-1)^n\binom{m+n-1}{n}\left(\frac{t - z_k}{z_k - z_j}\right)^n = g_j^m(z_k)\sum_{n=0}^{\infty}\binom{m+n-1}{n}\frac{g_k^n(z_j)}{g_k^n(t)} \tag{21}$$

Taking into account that $g_k^n(t)\overline{g_k^n(t)} = 1$, we get

$$\overline{g_j^m(t)} = \overline{g_j^m(z_k)}\sum_{n=0}^{\infty}\binom{m+n-1}{n}\overline{g_k^n(z_j)}g_k^n(t) \tag{22}$$

As a result, each term in the expansions of $g_j^m(t)$ and $\overline{g_j^m(t)}$ is a function of $g_k(t)$. Substituting Eqs. (21) and (22) into Eq. (13) and grouping the terms that are of the same power of $g_k(t)$, we obtain the following equations for $t \in L_k$, $(k = 1,\ldots,N)$

$$\sum_{m=2}^{M_k} mD_{mk}g_k^{1-m}(t)+\sum_{n=1}^{\infty}\sum_{\substack{j=1\\ j\neq k}}^{N}\frac{R_k}{R_j}\frac{g_k^n(z_j)}{g_k^n(t)}\sum_{m=1}^{M_j} m\binom{m+n}{n}D_{-mj}g_j^{m+1}(z_k)+2\,\mathrm{Re}(D_{1k})+\sum_{\substack{j=1\\ j\neq k}}^{N}\frac{R_k}{R_j}\sum_{m=1}^{M_j} m\Big[D_{-mj}g_j^{m+1}(z_k)$$

$$+\bar{D}_{-mj}\overline{g_j^{m+1}(z_k)}\Big]+\sum_{m=1}^{M_k} mD_{-mk}g_k^{m+1}(t)+\sum_{n=1}^{\infty}\sum_{\substack{j=1\\ j\neq k}}^{N}\frac{R_k}{R_j}\overline{g_k^n(z_j)}g_k^n(t)\sum_{m=1}^{M_j} m\binom{m+n}{n}\bar{D}_{-mj}\overline{g_j^{m+1}(z_k)}+\sum_{n=0}^{\infty}\sum_{\substack{j=1\\ j\neq k}}^{N}\frac{R_k}{R_j}\overline{g_k^n(z_j)}$$

$$\times\left\{g_k^{n+2}(t)\left[2(n+1)\mathrm{Re}(D_{1j})\overline{g_j^2(z_k)}+\sum_{m=2}^{M_j} m\binom{m+n}{n}D_{mj}\overline{g_j^{m+1}(z_k)}-\sum_{m=1}^{M_j} m(m+2)\binom{m+n+2}{n}\bar{D}_{-mj}\overline{g_j^{m+3}(z_k)}\right.\right.$$

$$\left.\left.+\sum_{m=1}^{M_j} m(m+1)\binom{m+n+1}{n}\bar{D}_{-mj}\frac{\overline{g_j^{m+2}(z_k)}}{g_j(z_k)}\right]-g_k^{n+1}(t)\sum_{m=1}^{M_j} m(m+1)\binom{m+n+1}{n}\bar{D}_{-mj}\overline{g_j^{m+1}(z_k)}\overline{g_k(z_j)}\right\}$$

$$=\left[\frac{\kappa+1}{4\mu}R_k(\sigma_{xx}^{\infty}+\sigma_{yy}^{\infty})-\frac{p_k}{\mu}R_k\right]-\frac{\kappa+1}{4\mu}R_k g_k^2(t)[(\sigma_{yy}^{\infty}-\sigma_{xx}^{\infty}-2\mathrm{i}\sigma_{xy}^{\infty})]-\frac{1-\kappa}{2\mu}R_k\sum_{n=0}^{\infty}(n+1)g_k^{n+2}(t)$$

$$\times\sum_{\substack{j=1\\ j\neq k}}^{N} p_j\overline{g_j^2(z_k)g_k^n(z_j)} \tag{23}$$

Now, both sides of this equation represent complex Fourier series and thus the complex coefficients for the terms of the same power must be equal. After neglecting the high order terms $g_k^n(t)$ for $n>M_k+1$ and $n<1-M_k$, Eq. (23) can be decomposed into a series of complex equations for $t\in L_k$ by equating the corresponding multiples of the same powers of $g_k(t)$.

By equating the coefficients of the positive powers $g_k^{\ell+1}(t)$ in $(1\le\ell\le M_k)$, the constant terms, and the negative powers $g_k^{1-\ell}(t)$ $(2\le\ell\le M_k)$ in Eq. (23), we obtain a system of $2M_k(k=1,\ldots,N)$ linear complex algebraic equations for all the Fourier coefficients

$$\mathrm{Re}(D_{1k})=-\frac{1}{2}\sum_{j=1,j\neq k}^{N}\frac{R_k}{R_j}\sum_{m=1}^{M_j} m[D_{-mj}g_j^{m+1}(z_k)+\bar{D}_{-mj}\overline{g_j^{m+1}(z_k)}]$$

$$+\frac{\kappa+1}{8\mu}R_k(\sigma_{xx}^{\infty}+\sigma_{yy}^{\infty})-\frac{p_k}{2\mu}R_k \tag{25}$$

$$D_{\ell k}=\sum_{j=1,j\neq k}^{N} g_k^{\ell}(z_j)\sum_{m=1}^{M_j}\binom{m+\ell-1}{\ell}D_{-mj}g_j^m(z_k), \tag{26}$$

$(\ell=2,\ldots,M_k)$

$$D_{-\ell k}=\sum_{\substack{j=1\\ j\neq k}}^{N}\overline{g_k^{\ell}(z_j)}\left\{\sum_{m=1}^{M_j}(\ell+1)\binom{m+\ell}{\ell+1}\bar{D}_{-mj}\overline{g_j^m(z_k)}\left[\frac{\overline{g_j(z_k)}}{g_j(z_k)}-\frac{m+\ell+1}{\ell+1}\overline{g_k^2(z_j)}-\frac{m+\ell+1}{m+1}\overline{g_j^2(z_k)}\right]+2\mathrm{Re}(D_{1j})\overline{g_j(z_k)}\right.$$

$$\left.+\sum_{m=2}^{M_j}\binom{m+\ell-l}{\ell}D_{mj}\overline{g_j^m(z_k)}\right\}+\begin{cases}-\dfrac{\kappa+1}{4\mu}R_k(\sigma_{yy}^{\infty}-\sigma_{xx}^{\infty}-2\mathrm{i}\sigma_{xy}^{\infty})-\dfrac{1-\kappa}{2\mu}R_k\displaystyle\sum_{j=1,\,j\neq k}^{N}p_j\overline{g_j^2(z_k)}, & (\ell=1)\\ -\dfrac{1-\kappa}{2\mu}R_k\displaystyle\sum_{j=1,\,j\neq k}^{N}p_j\overline{g_j^2(z_k)g_k^{\ell-1}(z_j)}, & (\ell=2,\ldots,M_k)\end{cases} \tag{24}$$

In the above procedure, it is observed that an infinite number of terms of the complex Fourier series gives the analytic solution for the given problem. This verifies that the approximation (6) is an accurate representation and the error only comes from the truncation.

4.5.2. Galerkin method

An alternative way to obtain a system of simultaneous linear algebraic equations for the overall problem is to use a Galerkin (weighted residual) method. In this method, both sides of each equation from the resulting complex system (13) are multiplied by selected weight functions, which are the powers of the function $g_k(t)$, and integrated along the boundaries. When evaluating the integrals, we use the orthogonality of the weight functions:

$$\oint_C g_k^m(t) g_k^n(t) \mathrm{d}t = \begin{cases} -2\pi \mathrm{i} R_k, & m+n=1 \\ 0, & m+n \neq 1 \end{cases} \tag{27}$$

where R_k is the radius of circle C and the ' $-$ ' sign indicates the clockwise traversal for holes.

The additional integrations required to implement the Galerkin procedure can also be performed analytically [14]. The linear system of complex algebraic equations obtained in this way is exactly the same as obtained above by using the Taylor series expansion.

4.5.3. Solution of the system

After separating the real and imaginary parts of the complex algebraic Eqs. (24)–(26), we obtain a real system of linear algebraic equations which can be written as

$$HX = G \tag{28}$$

where X is a vector of the real and imaginary parts of all the unknown complex coefficients D_{-mj}, D_{mj} in approximation (6); G is a known vector whose components depend on tractions acting on the holes and the stress conditions at infinity; and H is the coefficient matrix which can be written in $N \times N$ blocks

$$H = \begin{bmatrix} H_{11} & H_{12} & \cdots & H_{1N} \\ H_{21} & H_{22} & \cdots & H_{2N} \\ \cdots & \cdots & \cdots & \cdots \\ H_{N1} & H_{N2} & \cdots & H_{NN} \end{bmatrix} \tag{29}$$

where the submatrix H_{kj} $(k \neq j)$ expresses the influence of the jth hole on the kth hole. The individual terms of this submatrix are expressed in terms of elementary functions, which are functions of the distances between the centers of the kth and jth holes and their radii. As can be seen from Eqs. (24) to (26), the submatrix H_{kk} is an identity matrix corresponding to the kth hole.

The transposed vector of the unknowns X and right-hand side vector G in Eq. (28) can be written as

$$\begin{aligned} X^{\mathrm{T}} &= [\, X_1^{\mathrm{T}} \quad X_2^{\mathrm{T}} \quad \cdots \quad X_N^{\mathrm{T}} \,]; \\ G^{\mathrm{T}} &= [\, G_1^{\mathrm{T}} \quad G_2^{\mathrm{T}} \quad \cdots \quad G_N^{\mathrm{T}} \,] \end{aligned} \tag{30}$$

where X_k^{T} and G_k^{T} are, respectively, the transposed vector of unknowns and right-hand side vector for the kth hole.

The system (28) can be effectively solved by using a block Gauss–Seidel iteration algorithm. There is no need to store all elements of the matrix H in computer memory, because the submatrices H_{kj} can be easily recalculated during the iteration process. In the iterative procedure, we first compute the Fourier coefficients for given values M_k $(k = 1 \text{ to } N)$, and then increase the values of M_k until a specified degree of accuracy is achieved. Details about determining the number of terms in the Fourier expansion and the error estimation are given by Mogilevskaya and Crouch [14].

5. Numerical examples

5.1. Two circular holes in an infinite plane

As an example, we consider the case of two traction-free circular holes of different sizes in an infinite plane subjected to far-field stresses σ_{xx}^{∞}, σ_{yy}^{∞}, and σ_{xy}^{∞}. As shown in Fig. 2, two holes C_1 and C_2 with radii a and b are aligned with the x-axis and separated by a distance δ. The distance between the centers of the two holes is d. A point on boundary C_1 or C_2 is represented by θ_1 or θ_2 $(0^\circ \leq \theta_1, \theta_2 < 360^\circ)$.

The solution to this problem was given by Haddon [25] for the case of uniaxial tension at infinity. Haddon gave the results for different combinations of b/a and δ/a, and for different inclinations (0°, 45°, and 90°) of the applied tension. By using the numerical method described in this paper, we obtained results for $b/a = 5$ for the following two cases: (i) longitudinal tension ($\sigma_{xx}^{\infty} = 1.0$, $\sigma_{yy}^{\infty} = \sigma_{xy}^{\infty} = 0$)

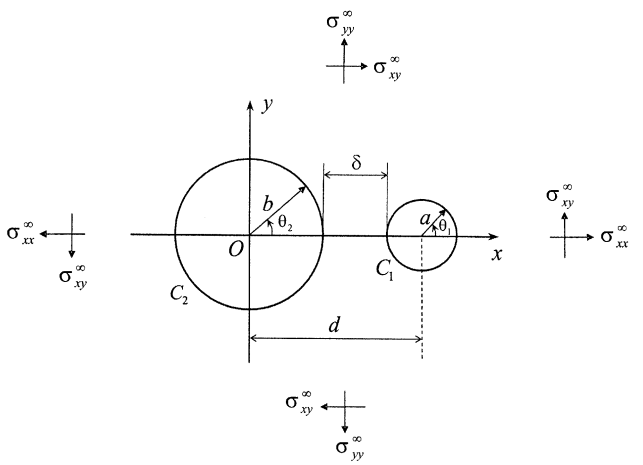

Fig. 2. Two circular holes in an infinite plane.

Table 1
Maximum and minimum stresses on C_1 and C_2 in Fig. 2 ($b/a = 5$ and $\sigma^{\infty}_{xx} = 1.0$)

δ/a	Present method				Haddon			
	σ_1	θ_1	σ_2	θ_2	σ_1	θ_1	σ_2	θ_2
0.1	0.403	77.8	3.005	89.7	0.403	77.8	3.005	89.7
	−4.577	180.0	−2.454	4.0	−4.577	180.0	−1.222	0.0
0.4	0.597	75.3	3.003	89.8	0.597	75.3	3.003	89.8
	−1.946	180.0	−1.271	7.3	−1.946	180.0	−1.011	180.0
1	0.819	73.8	3.000	90.0	0.819	73.7	3.000	90.0
	−0.860	180.0	−1.004	180.0	−0.861	180.0	−1.004	180.0
4	1.543	80.4	2.990	90.2	1.543	80.4	2.990	90.2
	−0.527	0.0	−0.997	180.0	−0.527	0.0	−0.997	180.0
10	2.303	87.5	2.986	90.2	2.303	87.5	2.986	90.2
	−0.724	0.0	−0.995	180.0	−0.724	0.0	−0.995	180.0

and (ii) transverse tension ($\sigma^{\infty}_{yy} = 1.0$, $\sigma^{\infty}_{xx} = \sigma^{\infty}_{xy} = 0$) and results for $b/a = 5$ and 10 for the case (iii) pure shear ($\sigma^{\infty}_{xy} = 1.0$, $\sigma^{\infty}_{xx} = \sigma^{\infty}_{yy} = 0$). Tables 1 and 2 show the values and locations (in degrees) of the maximum and minimum circumferential stresses along the holes for cases (i) and (ii) for different values δ/a of separation of the two holes. In these two tables and the following Table 3, the maximum and minimum stresses on C_1 and C_2 are denoted by σ_1 and σ_2, respectively, and the corresponding locations are measured by θ_1 and θ_2. The first set of numbers for each value of δ/a gives the maximum stresses and their locations on the two holes and the second set gives the minimum stresses and their locations. Our results agree closely with Haddon's except for the minimum stresses for hole C_2 for $\delta/a = 0.1$ and $\delta/a = 0.4$ in case (i) and the maximum stresses for hole C_2 for $\delta/a = 0.1$ in case (ii). An independent calculation using a real variables boundary integral analog of the method presented in this paper [27] confirmed that Haddon's results are erroneous in these instances, most likely due to a misprint. Table 3 shows the results for case (iii), which was not considered by Haddon. We find that the maximum and minimum stresses on

Table 2
Maximum and minimum stresses on C_1 and C_2 in Fig. 2 ($b/a = 5$ and $\sigma^{\infty}_{xx} = 1.0$)

δ/a	Present method				Haddon			
	σ_1	θ_1	σ_2	θ_2	σ_1	θ_1	σ_2	θ_2
0.1	19.312	180.0	9.962	4.1	19.312	180.0	4.596	0.0
	−1.370	128.8	−1.034	88.0	−1.370	128.8	−1.034	88.0
0.4	9.590	180.0	5.226	7.7	9.590	180.0	5.226	7.7
	−1.035	105.1	−1.028	88.7	−1.035	105.1	−1.028	88.7
1	6.118	180.0	3.663	10.5	6.118	180.0	3.663	10.5
	−0.648	95.7	−1.021	89.2	−0.648	95.7	−1.021	89.2
4	3.480	180.0	3.016	180.0	3.480	180.0	3.016	180.0
	−0.432	88.4	−1.004	89.9	−0.432	88.4	−1.004	89.9
10	3.069	0.0	3.004	180.0	3.069	0.0	3.004	180.0
	−0.680	89.1	−0.995	90.1	−0.680	89.1	−0.995	90.1

Table 3
Maximum and minimum stresses on C_1 and C_2 in Fig. 2 ($\sigma^{\infty}_{xx} = 1.0$)

δ/a	$b/a = 5$				$b/a = 10$			
	σ_1	θ_1	σ_2	θ_2	σ_1	θ_1	σ_2	θ_2
0.1	5.601	311.0	4.114	357.3	4.218	314.9	4.002	135.0
	−5.601	49.0	−4.114	2.7	−4.218	45.1	−4.002	225.0
0.4	5.669	311.1	4.020	134.9	4.462	314.6	4.002	135.0
	−5.669	48.9	−4.020	225.1	−4.462	45.4	−4.002	225.0
1	5.643	311.7	4.025	134.8	4.783	314.3	4.003	135.0
	−5.643	48.3	−4.025	225.2	−4.783	45.7	−4.003	225.0
4	5.375	137.7	4.028	134.8	5.362	313.8	4.006	135.0
	−5.375	222.3	−4.028	225.2	−5.362	46.2	−4.006	225.0
10	4.717	136.0	4.026	315.6	5.246	136.1	4.007	135.0
	−4.717	224.0	−4.026	44.4	−5.246	223.9	−4.007	225.0

the boundaries do not vary much with the distance between the holes for the case of pure shear, especially for the larger hole.

In the particular case of two circular holes of equal size, the results obtained for the cases of longitudinal tension and transverse tension are the same as those obtained by Ling [26] and Haddon [25]. To reproduce Haddon's results in the same accuracy for the cases of $b/a = 1$, $\sigma^{\infty}_{xx} = 1.0$, we need only 11 and 23 terms of the Fourier series for $\delta/a = 1$ and $\delta/a = 0.1$, respectively. More recently, Helsing and Jonsson [13] reconsidered this problem by using the fast multipole method with a collocation formulation. They found that for the case of $\delta/a = 0.2$, 80 collocation points are needed to reproduce Haddon's results. With our approach, only 19 terms of the complex Fourier series are required to obtain the same accuracy.

5.2. A row of colinear holes

The next example, depicted in Fig. 3, is for a row of N (N is odd) equally spaced colinear circular holes along the x-axis in an infinite plane under far-field uniform stresses σ^{∞}_{xx} and σ^{∞}_{yy}. All of the holes are of radius a and are separated by a distance δ (the center to center distance is d). This problem was solved by Howland [28], Horii and Nemat-Nasser [10], and Isida and Igawa [1], but with an infinite number of

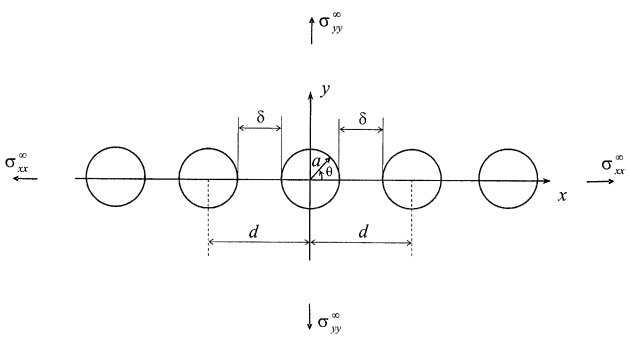

Fig. 3. A row of colinear holes in an infinite plane.

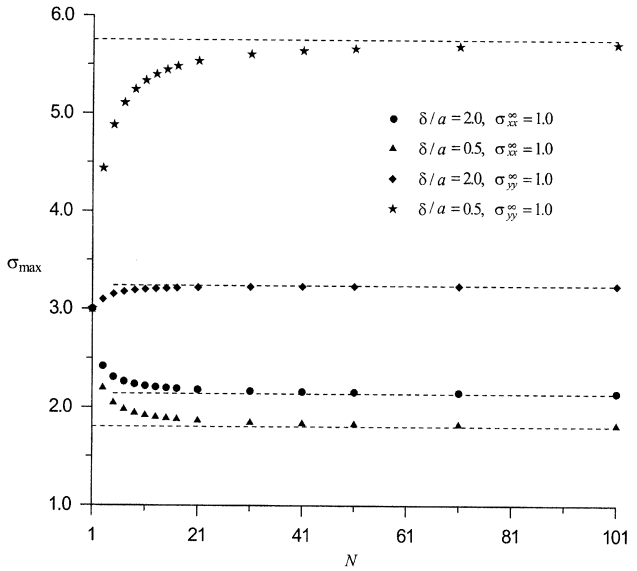

Fig. 4. Variation of the maximum circumferential stress along the central hole with the number N of colinear holes.

holes. The variations of the maximum circumferential stresses along the central hole with N for $\delta/a = 2$ and 0.5 for different loading cases are plotted in Fig. 4, in which the horizontal dotted lines denote the asymptotic solutions obtained by Horri and Nemat-Nasser [10] for an infinite number of holes. We find that our results approach the asymptotic solutions as N increases, especially for large value of δ/a. The influence of one hole on another falls off rapidly with the distance between them, and thus the interaction between the central hole and a noncentral one is insignificant and can be neglected as long as they are far enough apart.

Tables 4 and 5 show the results (in an accuracy of 10^{-4}) of maximum and minimum stresses on the boundary of the central hole for several combinations of N and δ/a for the cases of longitudinal tension ($\sigma^{\infty}_{xx} = 1.0$) and transverse tension ($\sigma^{\infty}_{yy} = 1.0$), respectively. For the cases we considered in Table 4, the maximum and minimum stresses occurred at $\theta = 0°$ and $\theta = 90°$, respectively, except for the cases $\delta/a \leq 1.0$, where the locations of the minimum stresses vary with different values of N and δ/a. For example, the locations of the minima for $N = 101$ for $\delta/a = 1.0$, 0.5, 0.2, and 0.1 are at $\theta = 18$, 26, 31, and 33°, respectively. For all the cases considered in Table 5, the locations of the maxima and minima are at $\theta = 90°$ and $\theta = 0°$, respectively. Upon comparing the results obtained by the present method for different finite numbers N with Horii and Nemat-Nasser's results for an infinite number of holes ($N = \text{inf}$) for the cases that $\delta/a = 18$, 8, 3, 2, 0.5 (which correspond to the cases $2a/d = 0.1$, 0.2, 0.4, 0.5, 0.8 in Horii and Nemat-Nasser [10]), we find that the two sets of results agree closely for large N except for the minimum stress for the case that $\delta/a = 0.5$. It is most likely that the value given by Horri and Nemat-Nasser for this instance is the stress at $\theta = 0°$, but not the minimum stress at $\theta = 26°$.

Table 4
Maximum and minimum stresses on the central hole ($\sigma^{\infty}_{xx} = 1.0$)

δ/a	$N = 11$		$N = 21$		$N = 41$		$N = 101$		$N = \text{inf}$ (Horii)	
	σ_{max}	σ_{min}	σ_{max}	σ_{min}	σ_{max}	σ_{min}	σ_{max}	σ_{min}	σ_{max}	σ_{min}
0.1	1.834	−0.391	1.773	−0.230	1.739	−0.124	1.717	−0.091	n/a	n/a
0.2	1.854	−0.212	1.796	−0.138	1.763	−0.113	1.742	−0.096	n/a	n/a
0.5	1.917	−0.179	1.864	−0.145	1.835	−0.126	1.815	−0.113	1.8018	−0.0029
1	2.021	−0.196	1.974	−0.172	1.948	−0.159	1.931	−0.150	n/a	n/a
2	2.219	−0.427	2.182	−0.408	2.161	−0.398	2.148	−0.391	2.1392	−0.3866
3	2.390	−0.603	2.360	−0.587	2.344	−0.579	2.333	−0.574	2.3261	−0.5699
8	2.792	−0.888	2.780	−0.882	2.774	−0.879	2.770	−0.877	2.7676	−0.8759
18	2.943	−0.971	2.940	−0.969	2.938	−0.969	2.937	−0.968	2.9363	−0.9676

Table 5
Maximum and minimum stresses on the central hole ($\sigma^{\infty}_{xx} = 1.0$)

δ/a	$N = 11$		$N = 21$		$N = 41$		$N = 101$		$N = \text{inf}$ (Horii)	
	σ_{max}	σ_{min}	σ_{max}	σ_{min}	σ_{max}	σ_{min}	σ_{max}	σ_{min}	σ_{max}	σ_{min}
0.1	16.814	−0.828	18.955	−0.722	20.276	−0.653	21.124	−0.607	n/a	N/a
0.2	9.972	−0.749	10.772	−0.670	11.230	−0.623	11.514	−0.592	n/a	N/a
0.5	5.335	−0.668	5.536	−0.619	5.644	−0.591	5.711	−0.574	5.7553	−0.5617
1	3.784	−0.634	3.852	−0.601	3.888	−0.583	3.910	−0.571	n/a	N/a
2	3.199	−0.659	3.219	−0.637	3.230	−0.625	3.237	−0.618	3.2411	−0.6124
3	3.078	−0.718	3.087	−0.701	3.091	−0.692	3.094	−0.687	3.0961	−0.6828
8	3.005	−0.898	3.006	−0.892	3.006	−0.889	3.006	−0.887	3.0063	−0.8853
18	3.000	−0.972	3.000	−0.970	3.000	−0.969	3.000	−0.969	3.0004	−0.9682

For the cases that $\delta/a = 1$, 0.2, and 0.1, the results are not available (n/a) in Horii and Nemat-Nasser [10].

5.3. A zig-zag array of circular holes

In this example, we analyze an array of circular holes in an infinite plane under uniaxial tension σ_0 in the y direction at infinity, as shown in Fig. 5. The center of the central hole in the array is located at the origin. All of the holes have radius a and are uniformly spaced in both the x and y directions. The center-to-center distances between the adjacent holes in horizontal and vertical rows are $2b$ and $2c$, respectively. This problem is patterned after several examples given by Isida and Igawa [1] for a periodic zig-zag array of circular holes in an infinite plane. Isida and Igawa solved this problem numerically by using a method based on element-wise resultant forces and displacements for two triangular and rectangular 'unit regions.' The same problem was solved by Ting et al. [30] for a finite number of holes by using the alternating method.

By using the present approach, we consider the problem of a finite array of N circular holes distributed in a zig-zag pattern inside a representative $S \times S$ square area (Fig. 6). The hole located at the center of this area is the one of interest. The numerical results depend upon the following two dimensionless parameters

$$\eta = \frac{c}{b}, \qquad \lambda = \frac{a}{b}$$

To study the influence of the surrounding holes on the central one, we consider four different values of S : $20a/3$, $40a/3$, $20a$, and $40a$ for the case of $\eta = 1.0$ and $\lambda = 0.6$. The number of holes calculated in the area considered are accordingly 13, 41, 85, and 313. The results of the normalized circumferential stresses on the boundary of the central hole obtained by using the present method are plotted in Fig. 7. Our calculations show that the influence of the surrounding holes that are far apart from the center of the area on the central hole is negligible, and that there is no significant change of the stress distribution along the central hole when the number of holes increases.

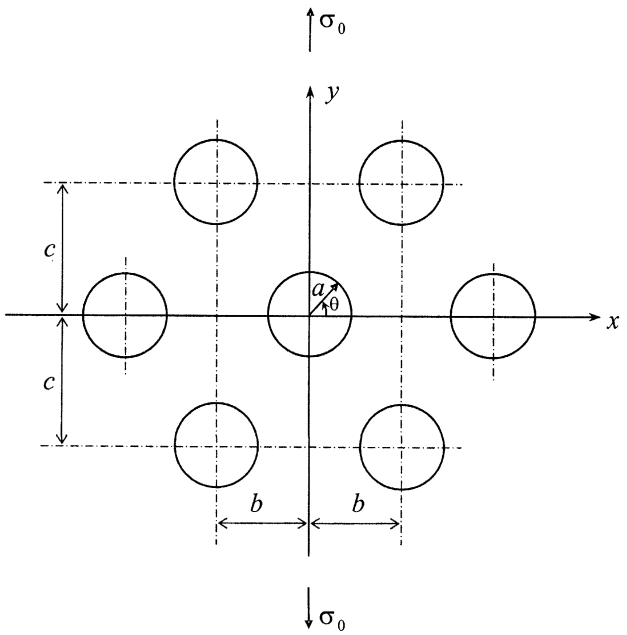

Fig. 5. A zig-zag array of circular holes in an infinite plane subjected to uniaxial tension.

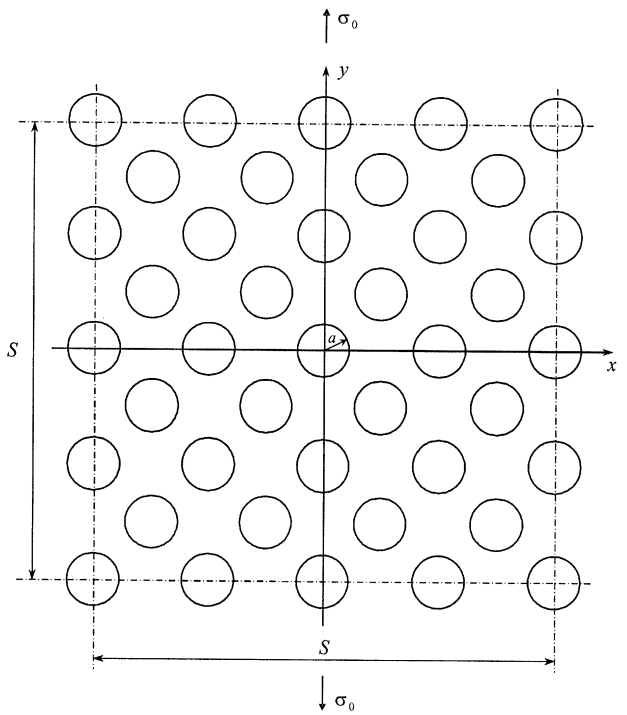

Fig. 6. Periodic distribution of circular holes in a zig-zag pattern inside the representative area.

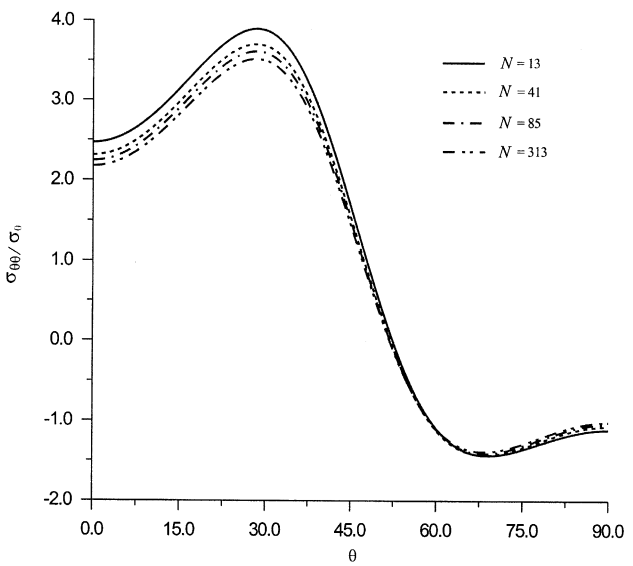

Fig. 7. Results of the normalized circumferential stress ($\sigma_{\theta\theta}/\sigma_0$) on the central hole with different numbers of surrounding holes for $\lambda = 0.6$ and $\eta = 1.0$.

Table 6
Maximum normalized stresses (σ_{max}/σ_0) on the central hole, compared with those for a doubly periodic system

λ	$\eta = 2.0$		$\eta = 1.0$		$\eta = 0.5$	
	Present	Isida	Present	Isida	Present	Isida
0.1	2.989	3.017	3.060	3.099	2.989	3.058
0.2	2.977	3.063	3.229	3.416	3.054	3.386
0.3	2.934	3.132	3.456	4.016	3.453	4.470
0.4	2.863	3.218	3.583	5.030	4.284	7.735
0.5	2.753	3.340	3.419	7.005		
0.6	2.657	3.576	3.519	15.710		
0.7	2.645	4.156				
0.8	2.886	5.707				

The above observation may lead one into an illusion that the result of the central hole in a sufficient large area is accurate enough to represent that of the case of an infinite array. Actually, the doubly periodic system behaves quite differently from one-dimensional periodic system and can never be approximated by a finite array. As an illustration, we reconsider the case of a finite array of circular holes distributed in an area of $40a \times 40a$. Three different values of η : 2.0, 1.0, and 0.5 are considered. To keep the adjacent holes from overlapping one another, the physical limits of λ for these three cases are 1.0, $\sqrt{2}/2$, and 0.5, respectively. The maximum values of λ we considered, however, are 0.8, 0.6, and 0.4, and the corresponding maximum number of holes we calculated in the area considered for these three cases are 281, 313, and 281. For these three worst cases, the maximum numbers of terms of the Fourier series required to achieve an accuracy of 10^{-4} are 33, 47, and 39, respectively. The maximum values of the circumferential stresses on the boundary of the central hole for different combinations of η and λ are given in Table 6. The results

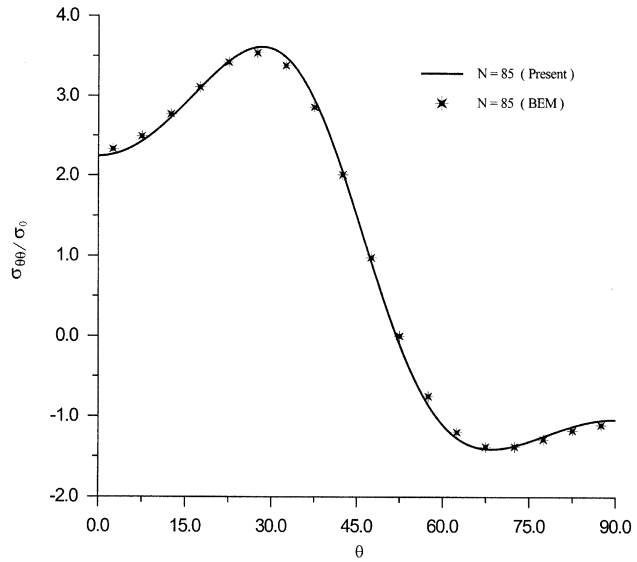

Fig. 8. Results of the normalized circumferential stress ($\sigma_{\theta\theta}/\sigma_0$) on the central hole from the present method and the boundary element method (BEM) for $N = 85$, and $\lambda = 0.6$, $\eta = 1.0$.

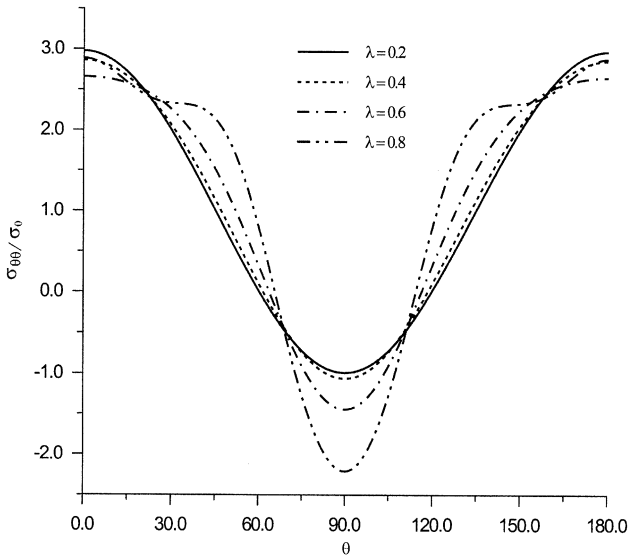

Fig. 9. Normalized circumferential stress ($\sigma_{\theta\theta}/\sigma_0$) on the central hole for discrete values of λ for the case of $\eta = 2.0$.

differ markedly from those for a doubly periodic system obtained by Isida and Igawa [1], especially for large values of λ. As an additional check on our results, we used a conventional boundary element method [29] to model the case for which $\eta = 1.0$ and $\lambda = 0.6$. For this analysis, 85 holes were modeled, with the central hole is discretized into 72 linear elements and each of the surrounding holes into 36 linear elements. The distribution of the circumferential stress along a quarter of the central hole is plotted in Fig. 8. It is found that the result from the boundary element method agrees closely with that obtained from the present method. Moreover, comparison of our results with those from Ting et al. [30] shows good agreement. From the above illustration, one can reach the conclusion that an approach

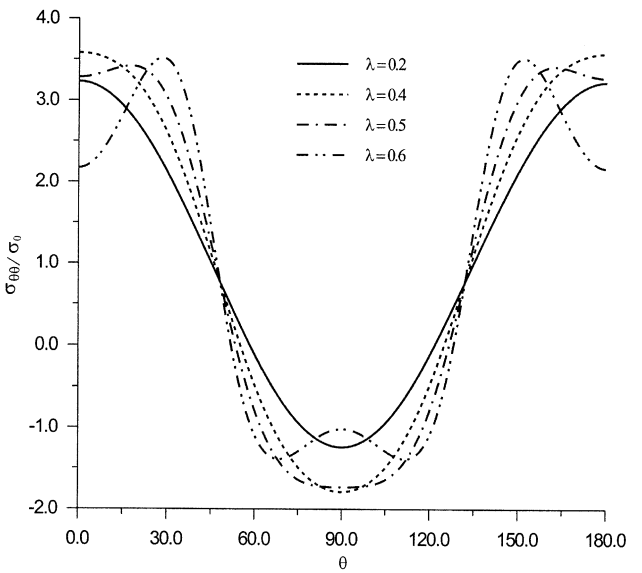

Fig. 10. Normalized circumferential stress ($\sigma_{\theta\theta}/\sigma_0$) on the central hole for discrete values of λ for the case of $\eta = 1.0$.

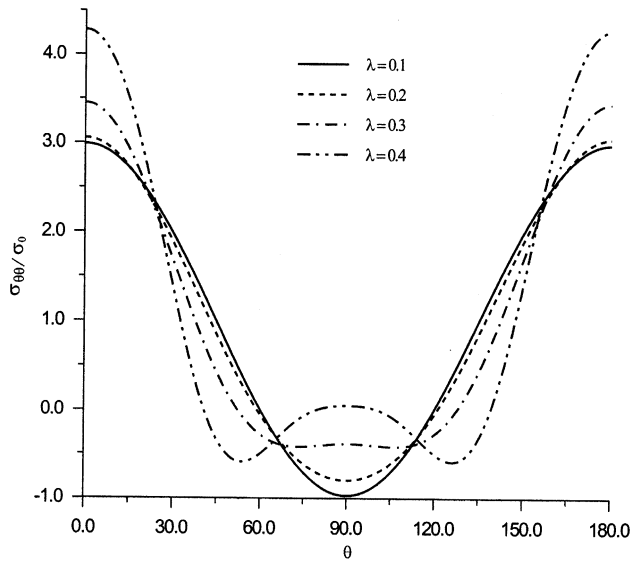

Fig. 11. Normalized circumferential stress ($\sigma_{\theta\theta}/\sigma_0$) on the central hole for discrete values of λ for the case of $\eta = 0.5$.

that assumes a periodic distribution of holes for a finite array may overestimate the interaction effect, especially when the holes are very close together.

In Table 6, most of maximum values are obtained at $\theta = 0°$ and 180°, except for two cases—$\eta = 1.0$, $\lambda = 0.5$ and $\eta = 1.0$, $\lambda = 0.6$—where the locations of the maximum stresses are 18 and 28°, respectively. Figs. 9–11 show the distributions of the normalized circumferential stresses $\sigma_{\theta\theta}/\sigma_0$ on the central hole for $\eta = 2.0$, 1.0 and 0.5. For small values of λ, the maximum and minimum boundary values of $\sigma_{\theta\theta}$ on the central hole occur at $\theta = 0°$ and 90°, while for large values of λ the locations of the maxima and minima depend on the values of η. For example, for $\eta = 1.0$, the location of $(\sigma_{\theta\theta})_{\max}$ shifts from $\theta = 0°$ with the increase of λ; for $\eta = 0.5$, the location of $(\sigma_{\theta\theta})_{\min}$ shifts from $\theta = 90°$. These variations show that the interactive effects between the holes in the horizontal and vertical rows change with different values of η and λ.

5.4. Multiple randomly distributed holes

As a final example, we demonstrate the use of our method for solving problems involving multiple randomly distributed holes. Fig. 12 shows contours of σ_{xx} in a plane with multiple holes subjected to uniform uniaxial tension $\sigma^{\infty}_{xx} = 1.0$ and uniform pressure $p = -1.0$ on three holes. The solution to this problem took less than one minute on a 900 MHz PC. Even though this problem only involves 11 holes, our approach can be used to solve more complicated

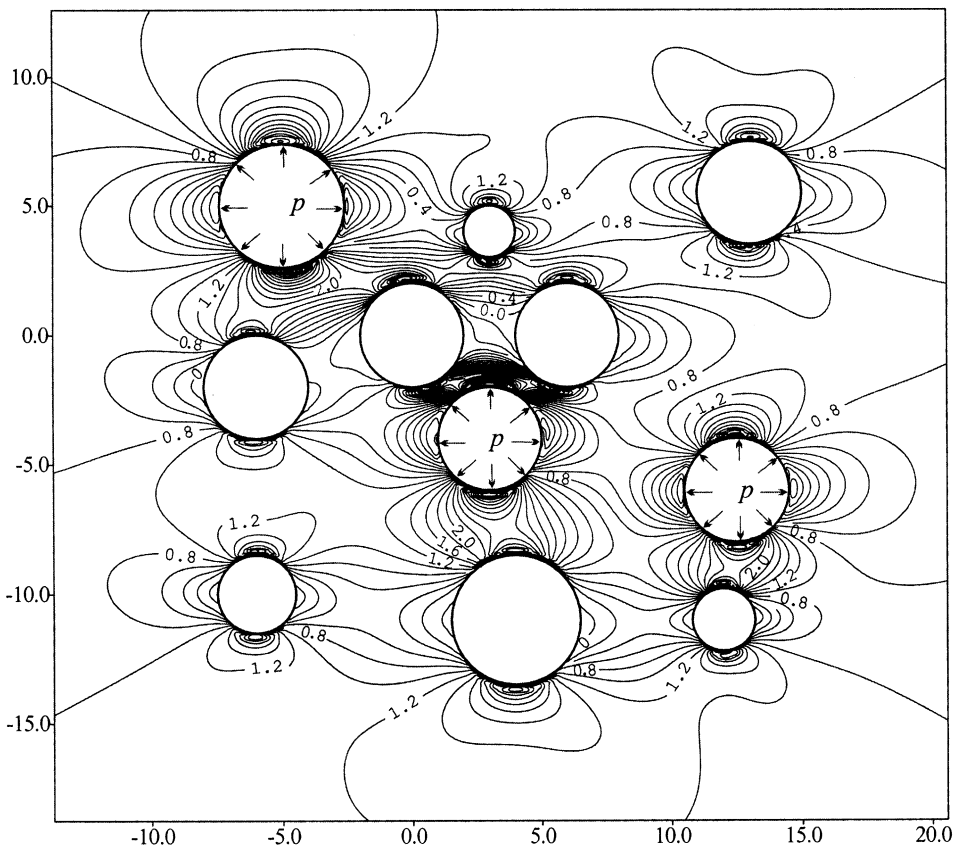

Fig. 12. Contours of σ_{xx} in a plate with multiple randomly distributed holes subjected to uniaxial tension at infinity ($\sigma^{\infty}_{xx} = 1.0$) and uniform pressure ($p = -1.0$) on several holes.

problems involving a large number of holes of arbitrary sizes and locations as long as none of the holes overlap.

During the process of solving the above problems, we found that the computation time strongly depends on the distances between the holes and variation of the hole sizes, because the numbers of terms in the associated Fourier series depend on these parameters. For holes that are relatively far apart, the stress field around them is not disturbed significantly and only a few terms of the truncated Fourier series are enough to give an accurate representation. For close-to-touching holes, more than twenty terms of the series are needed due to the strong interactions. Even for a large number of holes that are very close together, however, the problem can be efficiently solved by using the approach presented in this paper.

6. Conclusions

A numerical procedure based on a complex variable boundary integral equation and series expansion technique is presented for the problem of an infinite, isotropic elastic plane with multiple circular holes. A global representation of the unknown boundary parameters is used. The global representation requires no discretization of the boundaries, which avoids the most serious disadvantage of the collocation boundary element method. All of the singular and hypersingular integrals are evaluated analytically. The method shows that truncated complex Fourier series are good approximations of the unknown displacements at the boundaries of the circular holes. The accuracy, efficiency, and versatility of the method has been established through the numerical examples presented in the paper.

It is easy to incorporate multiple circular inclusions in the numerical method [31]. Other extensions are also possible, including the incorporation of cracks [32], elliptic inclusions and holes, and a finite external boundary. Work on these topics is in progress.

References

[1] Isida M, Igawa H. Analysis of a zig-zag array of circular holes in an infinite solid under uniaxial tension. Int J Solids Struct 1991;27(7): 849–64.
[2] Meguid SA, Kalamkarov AL, Yao J, Zougas A. Analytical, numerical, and experimental studies of effective elastic properties of periodically perforated materials. J Engng Mater Tech 1996;118:43–8.
[3] Green AE. General bi-harmonic analysis for a plate containing circular holes. Proc R Soc Lond 1940;A176:121–39.
[4] Yu I-W. Multiple circular inclusion problems in plane elastostatics. PhD Thesis, Case Western Reserve University, Cleveland, 1971
[5] Yu I-W, Sendeckyj GP. Multiple circular inclusion problems in plane elasticity. J Appl Mech 1974;41:215–21.
[6] Sokolnikoff IS. Mathematical theory of elasticity. New York: McGraw-Hill; 1956.
[7] Ting K, Chen KT, Yang WS. Applied alternating method to analyze the stress concentration around interacting multiple circular holes in an infinite domain. Int J Solids Struct 1999;36:533–56.
[8] Meguid SA, Shen CL. On the elastic fields of interacting defense and main hole systems. Int J Mech Sci 1992;34:17–29.
[9] Gong SX, Meguid SA. Interacting circular inhomogeneities in plane elastostatics. Acta Mech 1993;99:49–60.
[10] Horii H, Nemat-Nasser S. Elastic fields of interacting inhomogeneities. Int J Solids Struct 1985;21:731–45.
[11] Duan ZP, Kienzler R, Herrmann G. An integral equation method and its application to defect mechanics. J Mech Phys Solids 1986;34: 539–61.
[12] Greengard L, Helsing J. On the numerical evaluation of elastostatic fields in locally isotropic two-dimensional composites. J Mech Phys Solids 1998;46:1441–62.
[13] Helsing J, Jonsson A. Complex variable boundary integral equations for perforated infinite planes. Engng Anal Bound Elem 2001;25: 191–202.
[14] Mogilevskaya SG, Crouch SL. A Galerkin boundary integral method for multiple circular elastic inclusions. Int J Numer Meth Engng 2001; 52:1069–106.
[15] Mogilevskaya SG, Crouch SL. A Galerkin boundary integral method for multiple circular elastic inclusions with homogeneously imperfect interfaces. Int J Solids Struct 2002;39(18):4723–46. (b) Mogilevskaya SG, Crouch SL. Erratum. Int J Solids Struct 2003;40:1335.
[16] Nisitani H, Chen DH. Body force method and its applications to numerical and theoretical problems in fracture and damage. Comput Mech 1997;19(6):470–80.
[17] Rokhlin V. Rapid solution of integral equations of classical potential theory. J Comput Phys 1985;60:187–207.
[18] Greengard L, Rokhlin V. A fast algorithm for particle simulations. J Comput Phys 1987;73:325–48.
[19] Carrier J, Greengard L, Rokhlin V. A fast adaptive multipole algorithm for particle simulations. SIAM J Sci Stat Comput 1988;9: 669–86.
[20] Linkov AM, Mogilevskaya SG. Complex hypersingular integrals and integral equations in plane elasticity. Acta Mech 1994;105:189–205.
[21] Hromadka TV. The complex variable boundary element method in engineering analysis. New York: Springer-Verlag; 1987.
[22] Chen JT, Chen YW. Dual boundary element analysis using complex variables for potential problems with or without a degenerate boundary. Engng Anal Bound Elem 2000;24:671–84.
[23] Muskhelishvili NI. Some basic problems of the mathematical theory of elasticity. Groningen: Noordhoff; 1963.
[24] Linkov AM. Plane problems of the static loading of a piecewise homogeneous linearly elastic medium. J Appl Math Mech 1983;47: 527–32.
[25] Haddon RA. Stresses in an infinite plate with two unequal circular holes. Q J Mech Appl Math 1967;20:277–91.
[26] Ling CB. On the stresses in a plate containing two circular holes. J Appl Phys 1948;19:77–82.
[27] Crouch SL, Mogilevskaya SG. On the use of Somigliana's formula and Fourier series for elasticity problems with circular boundaries. Int J Numer Meth Engng 2002; in press.
[28] Howland RCJ. Stresses in a plate containing an infinite row of holes. Proc R Soc Lond 1935;A148:471–91.
[29] Crouch SL, Starfield AM. Boundary element method in solid mechanics. London: George Allen and Unwin; 1983.
[30] Ting K, Chen KT, Yang WS. Stress analysis of the multiple circular holes with the rhombic array using alternating method. Int J Pressure Vessels Piping 1999;76:503–14.
[31] (a) Wang J, Mogilevskaya SG, Crouch SL. Numerical implementation of a Galerkin boundary integral method for elastic materials with circular inclusions and holes. Electron J Bound Elem 2002;. (b) Wang J, Mogilevskaya SG, Crouch SL. BETEQ 2001;(1):85–93.
[32] Wang J, Mogilevskaya SG, Crouch SL. A Galerkin boundary integral method for nonhomogeneous materials with cracks. In: Elsworth D, Tinucci J, Heasley K, editors. Rock mechanics in the national interest. Balkema; 2001. p. 1453–60.